

# Satellite-based assessment of large-scale land cover change in Asian arid regions in the period of 2001–2009

Jaecil Cho · Yang-Won Lee · Pat J.-F. Yeh ·  
Kyung-Soo Han · Shinjiro Kanae

Received: 9 November 2012 / Accepted: 28 August 2013 / Published online: 7 September 2013  
© Springer-Verlag Berlin Heidelberg 2013

**Abstract** Arid regions in Asia are commonly characterized by rapidly growing populations with limited land resources and varying rainfall frequencies under climatic change. Despite being one of the most important environmental challenges in Asia, the changing aridity in this region, particularly due to large-scale land cover change, has not been well documented. In this study, we used rainfall data and a new land heterogeneity index to identify recent trend in land cover changes in the Asian arid regions. The result indicates a significant decreasing trend of barren lands and an increasing trend of vegetated lands. Although the potential land cover change is commonly believed to be strongly sensitive to rainfall change, such sensitivity has not been observed during the nine-year period (2001–2009) analyzed. Through the analyses of two separate periods (2001–2005 and 2005–2009), the sensitivity of rainfall to land cover change in arid regions is found to be dependent on the initial spatial heterogeneity of

vegetated land cover. The approach used and the findings in this study represent an important step toward better understanding of large-scale land cover change in the Asian arid regions, and have the potential to predict future land cover change under various climate change scenarios.

**Keywords** Asian arid regions · Land cover change · Barren and vegetated areas · Rainfall

## Introduction

Changes in the vegetated land surface in the arid and semiarid ecosystems contribute to the carbon emissions to the atmosphere as a result of desertification and related vegetation destruction, increased soil erosion, and reduced carbon sinks (Tucker et al. 1986; Lal 2001). Further, increased surface albedo associated with these land cover changes may feedback to decrease rainfall through enhanced radiative cooling (Charney 1975; Wei and Fu 1999). This, in turn, can cause a further decrease in the potential vegetation cover that can be sustained in the dry lands (Fu 2003). Consequently, degraded arid lands lead to alteration in the local ecosystem services, including food, fuel, and water for humans and livestock, irrigation, and sanitation (Noy-Meir 1973; Wang and Eltahir 2000). In addition, land degradation in arid regions can impact neighboring ecosystems through dust storms resulting from wind-induced soil erosion, and thus can strongly influence ecological environments and associated socioeconomic activities (Prospero and Nees 1986).

The spatio-temporal variations of vegetated lands are important for understanding the dynamics of arid land cover changes (Turner et al. 2007) because the loss of vegetation cover is considered as one of the major causes

---

**Electronic supplementary material** The online version of this article (doi:10.1007/s12665-013-2778-0) contains supplementary material, which is available to authorized users.

---

J. Cho (✉) · Y.-W. Lee · K.-S. Han  
Department of Spatial Information Engineering, Pukyong  
National University, 45 Yongso Road, Nam-Gu, Busan 608-737,  
Republic of Korea  
e-mail: chojaecil@gmail.com

P. J.-F. Yeh  
Department of Civil and Environmental Engineering,  
National University of Singapore, 21 Lower Kent Ridge Road,  
Singapore 119077, Singapore

S. Kanae  
Department of Civil Engineering, Tokyo Institute of  
Technology, 2-12-1 O-okayama, Meguro-ku,  
Tokyo 152-8552, Japan

of land degradation (Sivakumar 2007). The dynamic expansion and contraction of vegetated (or barren) surface can be expected to occur in the marginal regions of arid areas. The barren lands are gradually transformed into sub-humid lands through placing side by side of contrasting environments (Reynolds et al. 2007). Recent variations of rainfall, as the most critical driver and constraint for vegetation growth particularly in the border regions of arid areas (Tucker et al. 1991; Hickler et al. 2005), have shown irregular patterns as a result of warming of the atmosphere (Huntington 2006). The natural ecosystems in these regions are thus more vulnerable to perturbations in environmental conditions (Kassas 1995), and this implies that these regions have higher potential for the changes in the spatial distribution of vegetated lands.

Despite its environmental significance, however, land cover change in the regions bordering the arid areas is not easy to detect, primarily due to the difficulty in defining monitoring areas because of irregular climatic variations and gradational margins of vegetated lands in these regions (Cressey 1960). Indeed, the arid areas have complex boundaries and terrains, and are commonly characterized by limited land resources and varying rainfall frequencies under climatic change (Geist and Lambin 2004). Previous investigations have mostly focused on selected case studies using sub-national surveys and ground-based biophysical observations on the local-to-regional scales (Geist and Lambin 2004). As satellite remote sensing data are increasingly used to monitoring the changes in ecosystems (Kerr and Ostrovsky 2003) over extensive areas, they provide a unique opportunity to supplement the deficiency of ground-based biophysical observations for large areas. The relationship between satellite measured indices of land greenness and rainfall patterns has often been used to investigate the climate-induced land degradation on the basis of limited water resource availability in arid or semi-arid ecosystems (Archer 2004; Evans and Geerken 2004; Herrmann et al. 2005). However, this relationship of rainfall to vegetation greenness alteration cannot always fully explain land cover changes in arid areas (Lo Seen et al. 1995; Tracol et al. 2006).

In this study, we investigate the recent changes in the marginal arid lands of Asia using satellite remote sensing imagery. The one-third of the total lands in Asia is occupied by the arid lands. Even though the land cover change is one of the most important environmental challenges in the Asian arid regions (Guo et al. 2002; Lioubimtseva et al. 2005; Karnieli et al. 2008), however, the large-scale characteristics of the aridity in these regions have not been well documented. Here, our aim is to provide the satellite-based observational evidence of recent land cover changes in the Asian arid regions. A proposed new index, the Land Heterogeneity Index (LHI), is utilized to better characterize land cover changes by taking into account of the spatial distribution of vegetation cover in arid

regions. The spatial pattern of the trend of the annual rainfall is compared with that of annual variations in land cover changes as characterized by LHI in the Asian arid regions during the period of 2001–2009.

## Materials and methods

### Previous satellite-based indicators

In previous studies utilizing satellite imagery, vegetation greenness indices and land cover type products are commonly used to detect land cover changes. The greenness indices (e.g., the Normalized Difference Vegetation Index (NDVI) and Enhanced Vegetation Index (EVI)) can perform adequately well as the indicators of greenness and degradation in sparsely vegetated areas (Helldén and Tottrup 2008; Friedl et al. 2010). However, when considering the arid or semi-arid areas bordering vegetated desert surfaces, the accuracy of these indices may decrease due to surface background contamination since they are not standardized spatially and temporally (Pettorelli et al. 2005; Jiang et al. 2006). Further, even though the EVI is the corrected greenness index from the distortion by soil reflection, its spatiotemporal variation is too weak to accurately identify land cover changes due to the sparse vegetation coverage in arid areas in general (Jiang et al. 2008). Therefore, it may not be effective to use only vegetation greenness indices to detect land cover changes in the desertified and sparsely vegetated land, and this is particularly true for the Asian arid regions with rather complex ecological and geographical characteristics.

Over the last three decades, considerable efforts have been made to derive global-scale land cover information from the available remote sensing data (e.g., Tucker et al. 1985; Herold et al. 2006), and a few specific algorithms for this purpose have been developed (e.g., Bartholomé and Belward 2005; Friedl et al. 2010). The data of the Collection 5 moderate resolution imaging spectroradiometer (MODIS) global land cover type product (MCD12Q1.005) for our study period (2001–2009) have just become available recently (Friedl et al. 2010; Ke et al. 2012). The product is based not only on EVI, but also on land surface temperature (LST) and the adjusted reflectance (NBAR) values using the nadir bidirectional reflectance distribution (Geist and Lambin 2004; Friedl et al. 2010). It is divided into 16 land cover types, as shown in Table 1. Although large discrepancies found between remote sensing land cover maps and field-based references are yet to be solved (Foody 2002; Herold et al. 2006; See and Fritz 2006), the Collection 5 product has an updated ensemble algorithm and ancillary datasets, and it is substantially improved from the previous Collection 4 product (see Friedl et al. 2010).

**Table 1** The definition of 16 general land cover types from the MODIS classification

No.	Class_name
1	Evergreen Needleleaf forest
2	Evergreen Broadleaf forest
3	Deciduous Needleleaf forest
4	Deciduous Broadleaf forest
5	Mixed forest
6	Closed Shrub lands
7	Open Shrub lands
8	Woody savannas
9	Savannas
10	Grasslands
11	Permanent wetlands
12	Croplands
13	Urban and built-up
14	Cropland/natural vegetation mosaic
15	Snow ice
16	Barren or sparsely vegetated

However, Friedl et al. (2010) recommended that the land cover change should not be inferred by differencing the Collection 5 product across the time, because on the global scale this product contains low quality, mainly due to the ecological approximation of the land classes (e.g., mixed forest and deciduous broadleaf forest; mixed grassland and open shrublands). However, the barren or sparsely vegetated types (No. 16 in Table 1) have higher accuracy definitely because of their high surface albedo and low greenness [see Table 3 in Friedl et al. (2010)].

**Land heterogeneity index (LHI)**

Land cover change is traditionally classified into two types: conversion and modification (Leemans and Zuidema 1995; Gunderson 2000). Conversion refers to the complete replacement of one land cover type with another type, whereas modification signifies a more subtle change that affects the characteristics of land cover without changing its overall classification. When using remote sensing imagery for detecting both conversion and modification, it is difficult to compare land cover imageries obtained at different times because of the uncertainty in land classification (Iwasa 2000; Geist and Lambin 2004).

Land cover modification and transition are significantly associated with the spatially adjacent progression of land cover changes (Cressey 1960; Geist and Lambin 2004). That is, the land cover change at a region is critically related to that at the neighboring regions such as the eight pixels surrounding the center pixel (Fig. 1). The land cover conditions in the neighboring regions can be an important indicator to the current or potential changes of a certain

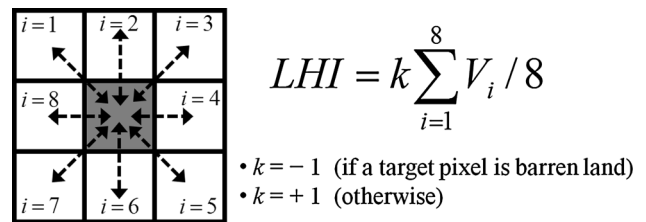


**Fig. 1** LHI computed from the average similarity value ( $V_i$ ) of the eight neighboring pixels surrounding a specific pixel (in gray). The value of  $V_i$  is given in Table 2

location (Cho et al. 2010). A similarity index, land heterogeneity index (LHI) at a location, is proposed and calculated as the average of the similarity value ( $V_i$ ) with regard to the eight nearest neighboring pixels (Fig. 1).  $V_i$  ranges from 0 to 1 depending on the similarity between a certain location and its neighboring pixels. It is 1.0 for the exactly identical land cover types and 0.0 for the completely different land cover types (see Table 2 for the look-up table of  $V_i$ ; Cho et al. 2010). Further, if the land cover type of a certain pixel is desert, the LHI is multiplied by  $-1$  to represent a negative value. Thus, LHI can range from  $-1.0$  to  $+1.0$ : negative values for the barren land and positive values for the vegetated land.

The index value of  $-1.0$  ( $+1.0$ ) indicates that a barren land (fully vegetated land) pixel is encompassed by the same land cover type, whereas the value between  $-1.0$  and  $+1.0$  indicates that the pixel is surrounded by different land cover types in some neighboring pixels (see Fig. S1 in Electronic Supplementary Material). Since the LHI is determined by neighboring pixels, it does not directly represent the land cover type of a certain pixel, except when LHI is  $-1.0$  or  $+1.0$ . The LHI signifies the potential condition of vegetated land at that time because it takes into account the similarity with the neighborhood types of land vegetation cover. If LHI is close to  $-1.0$  ( $+1.0$ ), the location has the largest tendency to retain its original status as a barren (vegetated) land, indicating a significantly desertified (steadily vegetated) state. Thus, LHI close to zero represents the most unstable state and often occurs on the transitory locations. The temporal variation in LHI can numerically represent land cover change in arid areas, and it is suitable to be used to continuously monitor the complex boundaries in the arid areas of Asia as a result of the highly variable climate conditions in these regions. The MODIS Collection 5 land cover type product (Collection 5) is satisfactory to calculate LHI due to high accuracy on the determination between barren and vegetated lands.

**Comparison of the trends of LHI and rainfall**

The variability in the spatial gradient of rainfall is often reflected as continuous changes in land vegetation cover.

**Table 2** The look-up table according to the MODIS land cover types (Table 1) to determine the similarity value ( $V_i$ ) for the calculation of LHI (Fig. 1)

	1	2	3	4	5	6	7	8	9	10	11	12	13	14	15	16
1	1.0	0.8	0.5	0.5	0.5	0.3	0.3	0.0	0.0	0.0	0.0	0.0	0.0	0.0	0.0	0.0
2	0.8	1.0	0.5	0.5	0.5	0.3	0.3	0.0	0.0	0.0	0.0	0.0	0.0	0.0	0.0	0.0
3	0.5	0.5	1.0	0.8	0.5	0.3	0.3	0.0	0.0	0.0	0.0	0.0	0.0	0.0	0.0	0.0
4	0.5	0.5	0.8	1.0	0.5	0.3	0.3	0.0	0.0	0.0	0.0	0.0	0.0	0.0	0.0	0.0
5	0.5	0.5	0.5	0.5	1.0	0.3	0.3	0.0	0.0	0.0	0.0	0.0	0.0	0.0	0.0	0.0
6	0.3	0.3	0.3	0.3	0.3	1.0	0.8	0.5	0.5	0.5	0.0	0.0	0.0	0.0	0.0	0.3
7	0.3	0.3	0.3	0.3	0.3	0.8	1.0	0.5	0.5	0.5	0.0	0.0	0.0	0.0	0.0	0.5
8	0.0	0.0	0.0	0.0	0.0	0.5	0.5	1.0	0.8	0.5	0.0	0.0	0.0	0.0	0.0	0.3
9	0.0	0.0	0.0	0.0	0.0	0.5	0.5	0.8	1.0	0.5	0.0	0.0	0.0	0.0	0.0	0.5
10	0.0	0.0	0.0	0.0	0.0	0.5	0.5	0.5	0.5	1.0	0.0	0.0	0.0	0.0	0.0	0.5
11	0.0	0.0	0.0	0.0	0.0	0.0	0.0	0.0	0.0	0.0	1.0	0.0	0.0	0.0	0.0	0.0
12	0.0	0.0	0.0	0.0	0.0	0.0	0.0	0.0	0.0	0.0	0.0	1.0	0.0	0.0	0.0	0.0
13	0.0	0.0	0.0	0.0	0.0	0.0	0.0	0.0	0.0	0.0	0.0	0.0	1.0	0.0	0.0	0.0
14	0.0	0.0	0.0	0.0	0.0	0.0	0.0	0.0	0.0	0.0	0.0	0.0	0.0	1.0	0.0	0.0
15	0.0	0.0	0.0	0.0	0.0	0.0	0.0	0.0	0.0	0.0	0.0	0.0	0.0	0.0	1.0	0.0
16	0.0	0.0	0.0	0.0	0.0	0.3	0.5	0.3	0.5	0.5	0.0	0.0	0.0	0.0	0.0	1.0

The product of 3B34 version 6 from the Tropical Rainfall Measuring Mission (TRMM), a joint U.S.–Japan satellite mission to monitor precipitation, is useful for large-scaled observation rainfall dataset (Berg et al. 2006). The 3B34 dataset with a  $0.25^\circ \times 0.25^\circ$  grid resolution is derived from the TRMM multi-satellite precipitation analysis (TMPA) and other satellite precipitation products, including the climate anomaly monitoring system (CAMS) global gridded rain gauge data produced by NOAA's Climate Prediction Center, and the global rain gauge product produced by the Global Precipitation Climatology Center (GPCC) (Kummerow et al. 1998). The target domain in the Asian arid regions corresponds to the pixels that are identified as barren lands (No. 16 in the MODIS land cover type list, see Table 1) more than once during the 2001–2009 period. The annual trends of LHI and rainfall ( $P$ ) at the pixels are calculated as the slope of the linear regression during the 2001–2009 period. For comparing the trends of LHI and  $P$ , monthly TRMM rainfall data are aggregated into annual time series. Further, the LHI grid has been converted from the sinusoidal map projection with a 500-m resolution into a geographic type of the  $0.25^\circ$  resolution to be consistent with the TRMM data.

## Results and discussion

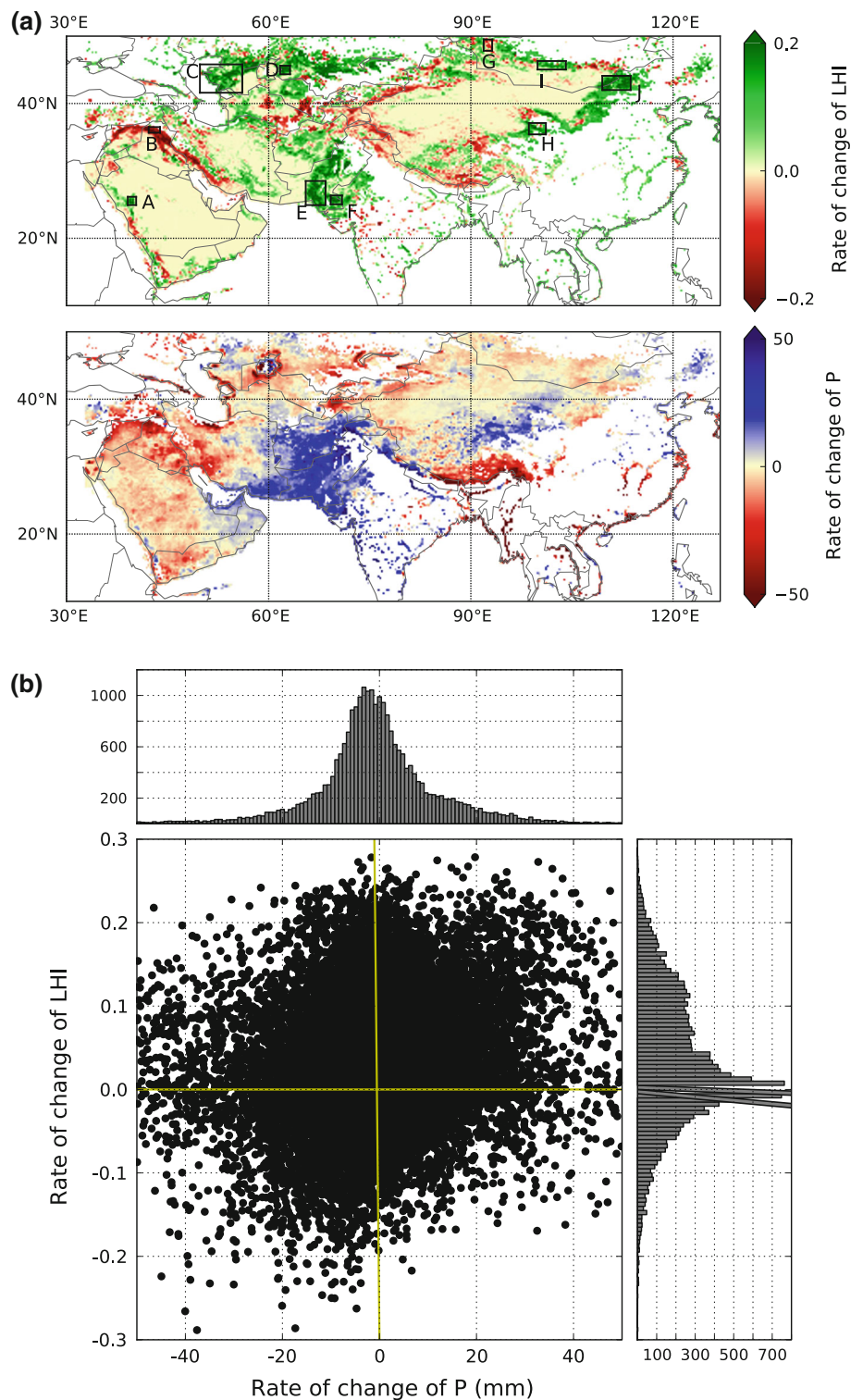
### Analysis of LHI and $P$ for the period of 2001–2009

Figure 2 shows the trend coefficients of the 2001–2009 annual LHI time series in Asian arid regions. A positive

trend (shown as green pixels in Fig. 2a) in LHI indicates a change from vegetated land to barren land, while a negative trend (red pixels) shows the change from degraded land to vegetated land. Across all the Asian arid regions, a positive trend in LHI is mostly found in the marginal areas, with the most remarkable arid regions in Pakistan, Kazakhstan, and the eastern parts of Inner Mongolia. On the other hand, a negative LHI trend is found in the western part of China, as well as the desert areas over Syria and Iraq. This finding is inconsistent with the common hypothesis that local desertification has increasingly happened due to human-induced pressure and adverse climatic effects (Agarwal 1979). However, the pattern shown in Fig. 2a is generally consistent with the green-up patterns over the global arid regions during the 1980s and 1990s reported by previous studies (e.g., Herrmann et al. 2005; Olsson et al. 2005; Helldén and Tottrup 2008).

The relationship between the trends in LHI and  $P$  can be expected to be positive because water is the limiting factor for plant growth in arid lands. The positive LHI trend (2001–2009) in Afghanistan, Pakistan, and northwest India is mostly associated with the increased  $P$ . Further, a negative trend (2001–2009) in both LHI and  $P$  can be found in the Tibet region and parts of Iraq and Iran. However, a positive correlation between the trends of LHI and  $P$  is not always found in the marginal areas of Asia. Among the four combinations of LHI and  $P$  (Fig. 2b), the number of pixels with an increasing LHI trend and a decreasing  $P$  trend is largest, whereas the number with a decreasing LHI trend associated with an increasing  $P$  trend is smallest. This implies that the variability in  $P$  cannot be considered

**Fig. 2** Spatial distribution of temporal trends in the land heterogeneity index (LHI) and annual total rainfall ( $P$ ) for 2001–2009 in the Asian arid regions. **a** Linear regression trends of LHI and  $P$ . *Green* and *red* colors represent the vegetating and desertification places in an arid area, respectively. *Yellow* regions show the unchanged land cover as a desert type. **b** Scatter plots between the trends of LHI and  $P$



as the solely dominant predictor of land cover changes in arid areas during the 2001–2009 period analyzed.

Since most land cover changes can be mainly attributed to both climatic and human influences, the following two cases, a positive trend in LHI with a negative trend in  $P$  and a negative trend in LHI with a positive trend in  $P$ , could be

regarded as a result of the more dominant influence of human activities than climate. However, there are complex interacting mechanisms affecting the response of large-scale land cover changes (Geist and Lambin 2004; Wessels et al. 2007) which are still under discussion (Herrmann and Hutchinson 2005). To identify human influences on land

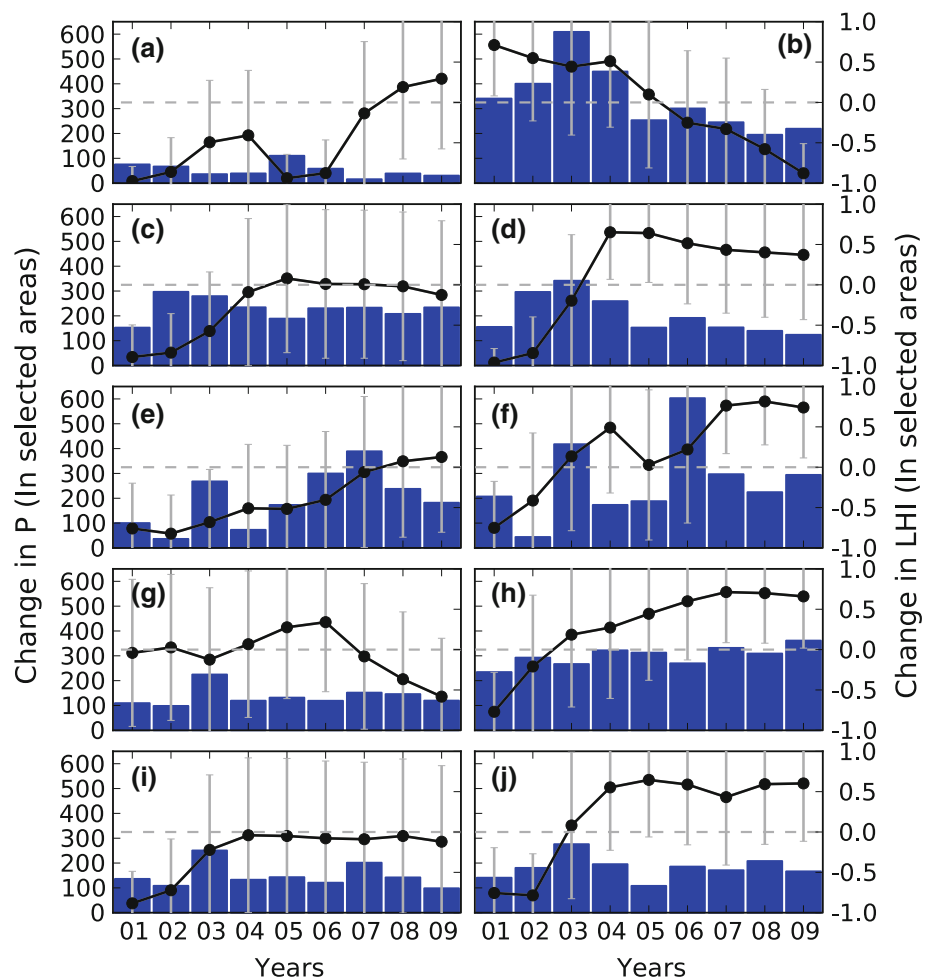
cover changes, the local causative factors have to be taken into account, but this may not be an easy task when dealing with the large-scale land cover changes as is the focus of this study. For example, a certain land that lies within a small area and has been seriously degraded or damaged by human activities (or by another local environmental factor) can be regarded as a highly affected region through local filed surveys, but it does not contribute to any dominant signals on the large-scaled land cover changes monitored by remote sensing.

#### Analysis of LHI and $P$ for the periods of 2001–2005 and 2005–2009

As plotted in Fig. 3, ten grid boxes (A–J shown in Fig. 2a) were selected to examine the relation between the temporal variations of annual LHI and  $P$ . Note that a clear correspondence between annual LHI to  $P$  variations is not expected because the response of land ecological conditions to  $P$  is highly nonlinear (MEA 2005). The LHI in the boxes A and F has a distinct positive trend throughout the whole period. The lands in both boxes were mostly barren

in 2001 and gradually changed into the vegetated state in 2004. However, in 2005 the land condition abruptly returned toward the barren condition in 2001 for the box A and near zero for the box F. After 2005, the vegetated areas started to increase again. While the LHI changes for both boxes A and F have a similar behavior, annual  $P$  variation of the box A has less change than that of box F. At least, rainfall change might not be the key reason of the LHI pattern in the box A. For the boxes C, D, I and J, the LHI were primarily increased during 2001–2005 (hereafter, as the Period I), and had little changes during 2005–2009 (hereafter as the Period II). Note that for the boxes D and J, LHI was about 0.5 during the Period II, while for C and I, it was nearly zero. If LHI is close to zero, the land cover tends to be most vulnerable to environmental changes due to the heterogeneous land conditions. The annual  $P$  changes of these four boxes were not relatively large, but all have higher rainfall during the Period I than Period II. For the box G, after a nearly zero LHI in the Period I, the land gradually changed toward the barren condition in the Period II. On the other hand, annual  $P$  is rather constant throughout the whole period. For the boxes E and H, the

**Fig. 3** Plots of LHI and  $P$  variations during 2001–2009 in ten selected land area



LHI continued to increase during the Period II. However, the annual  $P$  during the Period II of the box E is relatively larger than that during the Period I, whereas the  $P$  in both periods for the box H has almost no change. For the box B, the LHI was continuously decreased from  $\sim 1.0$  to  $\sim -1.0$  throughout the whole period. Similarly, the relatively larger rainfall in the Asian arid regions during the Period I became smaller during the Period II (see Fig. 4a, c).

The results from the analysis of nine-year LHI dataset reveal no simple temporal variation. We analyzed the spatial distribution of the trends in both LHI and  $P$  as well as the relation between them for the Period I and II,

separately. For the Period I, the comparison between Figs. 2a and 4a reveals that the pixels with a positive LHI trend during the Period I were dominantly spread out in the Asian arid regions than that during the entire 2001–2009 period. In contrast, for the Period II, the pixels with a negative trend in LHI were largely appeared, particularly from the Central Asia to Mongolia (Fig. 4c). The LHI trends in Central Asia, northwest China, and Mongolia in contrast were changed from rather positive for the Period I to rather negative for the Period II. However, the Pakistan and Inner Mongolia regions exhibited a positive trend in LHI during both periods, while the Tibet region changed

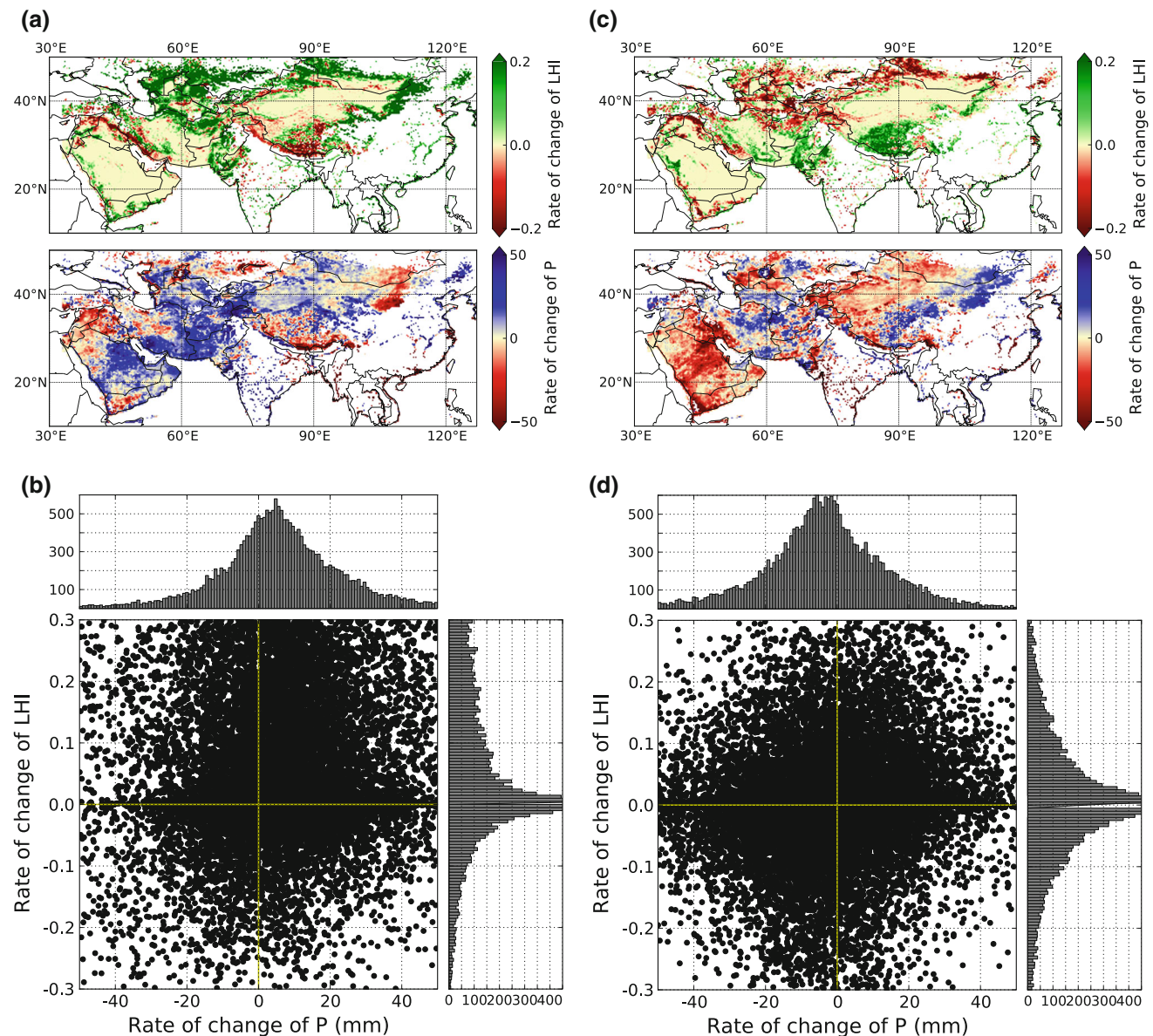


**Fig. 4** Spatial distribution of the temporal trends in LHI and  $P$  in the Asian arid regions during 2001–2005 (a, b) and 2005–2009 (c, d). a, c Linear regression trends of LHI and  $P$ . Green and red colors

represent the vegetated and desertification places in an arid area, respectively. Yellow regions show the unchanged land cover as a desert type. b, d Scatter plots between the trends of LHI and  $P$

from a negative to a positive trend in LHI from the Period I to Period II. The western part of the Taklamakan Desert consistently had a negative trend in both periods. The changes in LHI trend in the Arabian Peninsula and western Iran were not that different between two periods, and even changed from positive to negative in the bottom of the Arabian Peninsula. However, note that the spatial pattern of positive (negative) LHI trend in LHI is not always consistent with that of the positive (negative) trend in  $P$  (Figs. 4b, d).

Land cover changes continuously on the basis of the past vegetated condition (Iwasa 2000). To identify the effects of the past land condition on the sensitivity of LHI to  $P$ , the following four simple conceptual cases are considered here: the positive trends in both  $P$  and LHI (Case I), a negative trend in  $P$  and a positive trend in LHI (Case II), the negative trends in both  $P$  and LHI (Case III), and a positive trend in  $P$  and a negative trend in LHI (Case IV). Figure 5 shows the change in the  $P$ -LHI sensitivity from the Period I to Period II. Several interesting behaviors can be found across both the Period I to II. For example, there is less likely for any Case to be remained unchanged for the Period II. This probably implies the large variability in the environmental vegetation conditions. Case I is mainly changed to Case III among four cases. Further, Case III is also generally changed into Case I. When considering that the Cases I and III are the commonly expected patterns because of limited water resource availability in arid ecosystem, the higher transition between the Cases I and III signifies that the expected positive sensitivity of LHI to  $P$  changes mostly in a continuous fashion at a relatively long time scale. However, the probability for the Case III during Period I of changing into the Case I (30.7 %) is

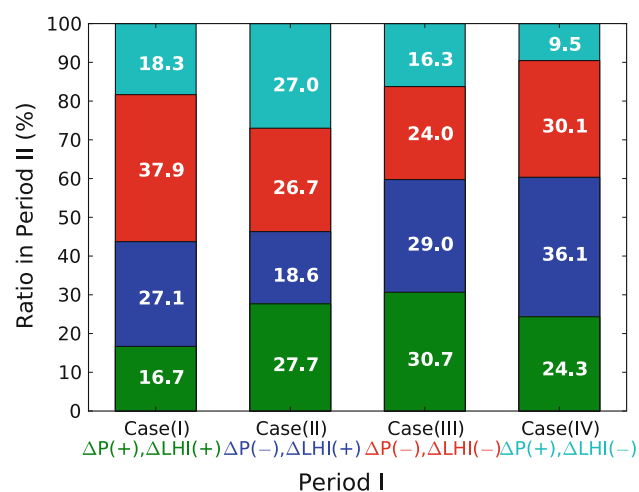


**Fig. 5** Changes noticed in the four cases for  $P$ -LHI sensitivity from the first period (Period I, 2001–2005) to the second period (Period II, 2005–2009). Color indicates each cases: the green for Case I, the blue for Case II, the red for Case III, and the cyan for Case IV

almost equal to that of changing into Case II (29.0 %). On the other hand, after the land condition in the Case II of the negative  $P$  pattern, the negative pattern of LHI is largely appeared during Period II (e.g., Cases III and IV). Further, the Case IV with the positive  $P$  pattern is mostly changed into the positive pattern of LHI (e.g., Cases I and II).

## Summary and conclusion

In this study, we use a new land heterogeneity index (i.e., LHI) and annual rainfall data to identify the trend and characteristics of land cover changes in the Asian arid regions over the 2001–2009 period. Although the LHI trend cannot be directly interpreted as the greening of arid lands, it can identify the growing potential for vegetation greenness. The dominant temporal patterns of the LHI trend over this period show significant disappearance of non-barren lands. In addition, the expected strong vegetation sensitivity to rainfall is not clearly observed in the nine-year period analyzed (2001–2009). However, through the analysis of two separated periods (2001–2005 and 2005–2009), we conclude that the rainfall sensitivity (i.e., the strength and time-lag of the response) of arid lands depends on the initial vegetated land condition. Accordingly, when considering the smaller annual rainfall amount for the period of 2005–2009 in comparison to the period of 2001–2005, the expansion of degraded land after 2009 should be considered without reference to the rainfall change, particularly in the Asian arid regions.

Climatic changes have made it imperative to conduct investigations into the situations and causes of arid land changes on the large spatial scale. Considering that large-scale land cover changes are mainly induced by a few major environmental factors rather than various local environmental conditions, more large-scale monitoring studies should provide insights into the cause-and-effect relationships and help enhance understanding of arid land changes. These studies can provide valuable information for climatic modeling. The altered land surface albedo in the desert areas certainly has an effect on global climatic changes through the feedback processes in the hydrometeorological cycle. For example, the dynamic global vegetation models (DGVM), which take into account the impacts of land cover changes on the water and carbon cycles, still require abundant measurement data for model validation or parameterization. Hence, further work is required for identifying the mechanisms of large-scale land cover changes in the arid regions under the continuing climate change conditions.

The policy making in the management of arid regions should be based on accurate spatial and temporal information of land cover changes because land is highly related



to human well-being and sustainable social development. In general, the local-scale approaches focus on the field observations and fine-scaled simulations, and their dynamics within the specific ecosystems, but the changes on the large scale are difficult to detect. Further, the mechanisms identified from the local-scale studies are difficult to extrapolate to larger scales. Therefore, the results presented in this study should be complemented using local-scale surveys and data collection for better predictions of future arid land changes.

**Acknowledgments** We would like to thank to editor and anonymous reviewers, whose comments were valuable for revising this manuscript. This study was partially supported by “Long-term Vision for the Sustainable Use of the World’s Freshwater Resources” program through Core Research for Evolutional Science and Technology (CREST) under the Japan Science and Technology Agency, Japan, and the Korea Meteorological Administration Research and Development Program under Grand CATER 2012-2066, Korea.

**References**

Agarwal A (1979) Why the world’s deserts are still spreading. *Nature* 277:167–168

Archer ERM (2004) Beyond the “climate versus grazing” impasse: using remote sensing to investigate the effects of grazing system choice on vegetation cover in the eastern Karoo. *J Arid Environ* 57:381–408

Bartholomé E, Belward AS (2005) GLC2000: a new approach to global land cover mapping from Earth observation data. *Int J Remote Sens* 26:1959–1977

Berg W, L’Ecuyer T, Kummerow C (2006) Rainfall climate regimes: the relationship of regional TRMM rainfall biases to the environment. *J Appl Meteor Climatol* 45:434–454

Charney JG (1975) Dynamics of deserts and drought in the Sahel. *Q J Roy Meteorol Soc* 101:193–202

Cho J, Yeh PJ-F, Lee Y-W, Kim H, Oki T, Kim W, Otsuki K (2010) A study on the relationship between Atlantic sea surface temperature and Amazonian greenness. *Ecol Informat* 5:367–378

Cressey GB (1960) The deserts of Asia. *J Asian Stud* 19:389–402

Evans J, Geerken R (2004) Discrimination between climate and human induced dryland degradation. *J Arid Environ* 57:535–554

Foody GM (2002) Status of land cover classification accuracy assessment. *Rem Sens Environ* 80:185–201

Friedl MA, Sulla-Menashe D, Tan B, Schneider A, Ramankutty N, Sibley A, Huang X (2010) MODIS Collection 5 global land cover: algorithm refinements and characterization of new datasets. *Rem Sens Environ* 114:168–182

Fu C (2003) Potential impacts of human-induced land cover change on East Asia monsoon. *Global Planet Change* 37:219–229

Geist HJ, Lambin EF (2004) Dynamic causal patterns of desertification. *Bioscience* 54:817–829

Gunderson LH (2000) Ecological resilience—in theory and application. *Annu Rev Ecol Systemat* 31:425–439

Guo ZT, Ruddiman WF, Hao QZ, Wu HB, Qiao YS, Zhu RX, Peng SZ, Wei JJ, Yuan BY, Liu TS (2002) Onset of Asian desertification by 22 Myr ago inferred from loess deposits in China. *Nature* 416:159–163

Helldén U, Tottrup C (2008) Regional desertification: a global synthesis. *Glob Planet Change* 64:169–176

Herold M, Woodcock C, Di Gregorio A, Mayaux P, Belward A, Latham J, Schmullius CC (2006) A joint initiative for harmonization and validation of land cover datasets. *IEEE Trans Geosci Rem Sens* 44:1719–1727

Herrmann SM, Hutchinson CF (2005) The changing contexts of the desertification debate. *J Arid Environ* 63:538–555

Herrmann SM, Anyamba A, Tucker CJ (2005) Recent trends in vegetation dynamics in the African Sahel and their relationship to climate. *Global Environ Change* 15:394–404

Hickler T, Eklundh L, Seaquist JW, Smith B, Ardö J, Olsson L, Sykes MT, Sjöström M (2005) Precipitation controls Sahel greening trend. *Geophys Res Lett*. doi:10.1029/2005GL024370

Huntington TG (2006) Evidence for intensification of the global water cycle: review and synthesis. *J Hydrol* 319:83–95

Iwasa Y (2000) Lattice models and pair approximation in ecology. In: Dieckmann U, Law R, Metz JAJ (eds) *The geometry of ecological interactions: simplifying spatial complexity*. Cambridge University Press, Cambridge, pp 227–251

Jiang ZY, Huete AR, Chen J, Chen YH, Li J, Yan GJ, Zhang XY (2006) Analysis of NDVI and scaled difference vegetation index retrievals of vegetation fraction. *Rem Sens Environ* 101:366–378

Jiang Z, Huete AR, Didan K, Miura T (2008) Development of a two-band enhanced vegetation index without a blue band. *Rem Sens Environ* 112:3833–3845

Karnieli A, Gilad U, Ponzet M, Svoray T, Mirzadinov R, Fedorina O (2008) Assessing land-cover change and degradation in the Central Asian deserts using satellite image processing and geostatistical methods. *J Arid Environ* 72:2093–2105

Kassas M (1995) Desertification: a general review. *J Arid Environ* 30:115–128

Ke Y, Leung LR, Huang M, Coleman AM, Li H, Wigmosta MS (2012) Development of high resolution land surface parameters for the community land model. *Geosci Model Dev* 5:1341–1362

Kerr JT, Ostrovsky M (2003) From space to species: ecological applications for remote sensing. *Trends Ecol Evol* 18:809–817

Kummerow C, Barnes W, Kozu W, Shiue T, Simpson J (1998) The tropical rainfall measuring mission (TRMM) sensor package. *J Atmos Ocean Tech* 15:809–817

Lal R (2001) Potential of desertification control to sequester carbon and mitigate the greenhouse effect. *Climatic Change* 51:35–72

Leemans R, Zuidema G (1995) Evaluating changes in land cover and their importance for global change. *Trends Ecol Evol* 10:76–81

Lioubimtseva E, Cole R, Adams JM, Kapustin G (2005) Impacts of climate and land-cover changes in arid lands of Central Asia. *J Arid Environ* 62:285–308

Lo Seen D, Mougin E, Rambal S, Gaston A, Hiernaux P (1995) A regional Sahelian grassland model to be coupled with multi-spectral satellite data. II: toward the control of its simulations by remotely sensed indices. *Rem Sens Environ* 52:194–206

MEA (Millennium Ecosystem Assessment) (2005) *Ecosystems and human well-being: desertification synthesis*. World Resources Institute, Washington DC. <http://www.millenniumassessment.org/documents/document.355.aspx.pdf>

Noy-Meir I (1973) Desert ecosystems: environment and producers. *Annu Rev Ecol Systemat* 4:51–58

Olsson L, Eklundh L, Ardö J (2005) A recent greening of the Sahel—trends, patterns and potential causes. *J Arid Environ* 63:556–566

Pettorelli N, Vik JO, Mysterud A, Gaillard J-M, Tucker CJ, Stenseth NC (2005) Using the satellite-derived NDVI to assess ecological responses to environmental change. *Trends Ecol Evol* 20: 503–510

Prospero JM, Nees RT (1986) Impact of the North African drought and El Niño on mineral dust in the Barbados Trade Winds. *Nature* 320:735–738

Reynolds JF, Stafford Smith DM, Lambin EF, Turner BL II, Mortimore M, Batterbury SPJ, Downing TE, Dowlatabadi H,

- Fernández RJ, Herrick JE, Huber-Sannwald E, Jiang H, Leemans R, Lynam T, Maestre FT, Ayarza M, Walker B (2007) Global desertification: building a science for dryland development. *Science* 316:847–851
- See L, Fritz S (2006) Towards a global hybrid land cover map for the year 2000. *IEEE Trans Geosci Rem Sens* 44:1740–1746
- Sivikumar MVK (2007) Interactions between climate and desertification. *Agric For Meteorol* 142:143–155
- Tracol Y, Mougin E, Hiernaux P, Jarlan L (2006) Testing a Sahelian grassland functioning model against herbage mass measurements. *Ecol Model* 193:437–446
- Tucker CJ, Townshend JRG, Goff TE (1985) African land-cover classification using satellite data. *Science* 227:369–375
- Tucker CJ, Fung IY, Keeling CD, Gammon RH (1986) Relationship between atmospheric CO<sub>2</sub> variations and a satellite-derived vegetation index. *Nature* 319:195–199
- Tucker CJ, Dregne HE, Newcomb WW (1991) Expansion and contraction of the Sahara desert from 1980 to 1990. *Science* 253:299–301
- Turner BL II, Lambin EF, Reenberg A (2007) The emergence of land change science for global environmental change and sustainability. *Proc Natl Acad Sci* 104:20666–20671
- Wang GL, Eltahir EB (2000) Role of vegetation dynamics in enhancing the low-frequency variability of the Sahel rainfall. *Water Resour Res* 36:1013–1021
- Wei H, Fu C (1999) Study of the sensitivity of a regional model in response to land cover change over northern China. *Hydrol Process* 12:2249–2265
- Wessels KJ, Prince SD, Malherbe J, Small J, Frost PE, VanZyl D (2007) Can human-induced land degradation be distinguished from the effects of rainfall variability? A case study in South Africa. *J Arid Environ* 68:271–297